

Seeking for sterile neutrinos with displaced leptons at the LHC

Jia Liu,¹ Zhen Liu,² Lian-Tao Wang,^{1,3} and Xiao-Ping Wang⁴

¹*Enrico Fermi Institute, University of Chicago, Chicago, IL 60637, USA*

²*Maryland Center for Fundamental Physics, Department of Physics,
University of Maryland, College Park, MD 20742, USA*

³*Kavli Institute for Cosmological Physics,
University of Chicago, Chicago, IL 60637, USA*

⁴*High Energy Physics Division, Argonne National Laboratory, Argonne, IL 60439, USA*

(Dated: July 29, 2019)

We study the signal of long-lived sterile neutrino at the LHC produced through the decay of the W boson. It decays into charged lepton and jets. The characteristic signature is a hard prompt lepton and a lepton from the displaced decay of the sterile neutrino, which leads to a bundle of displaced tracks with large transverse impact parameter. Different from other studies, we neither reconstruct the displaced vertex nor place requirement on its invariant mass to maintain sensitivity for low sterile neutrino masses. Instead, we focus on the displaced track from the lepton. A difficulty for low mass sterile neutrino study is that the displaced lepton is usually *non-isolated*. Therefore, leptons from heavy flavor quark is the major source of background. We closely follow a search for displaced electron plus muon search at CMS and study their control regions, which is related to our signal regions, in great detail to develop a robust estimation of the background for our signals. After further optimization on the signal limiting the number of jets, low H_T and large lepton displacement d_0 to suppress SM background, we reach an exclusion sensitivity of about 10^{-8} (10^{-5}) for the mixing angle square at 10 (2) GeV sterile neutrino mass respectively. The strategy we propose can cover the light sterile masses complimentary to beam dump and forward detector experiments.

CONTENTS

| | |
|---|----|
| I. Introduction | 2 |
| II. Sterile neutrino models | 3 |
| III. Sterile neutrino properties | 5 |
| IV. New searches strategy for sterile neutrinos | 8 |
| V. Conclusion and outlook | 16 |
| References | 19 |

I. INTRODUCTION

The origin of the neutrino masses is a puzzle of the Standard Model [1–4]. The parameters in the neutrino sector, such as the mass differences and mixing angles, have been measured with higher and higher precision [5]. At the same time, cosmological observations set an upper bound on the sum of neutrino masses to be smaller than 0.12 eV and the effective extra relativistic degrees of freedom to be $N_{\text{eff}} = 2.99 \pm 0.17$ from Planck 2018 data [6]. Many mechanisms have been introduced to incorporate the presence of the tiny neutrino masses. Among them, the seesaw type of solutions to the small neutrino mass is probably the most plausible. A heavier, often sterile, neutrino to realize the seesaw mechanism of a certain type would be a smoking gun signal for this class of models.

Many active experimental programs have been developed to search for sterile neutrinos, through oscillation via light (eV-keV) ones at current or future short and long-baseline neutrino facilities [7–12], neutrinoless double-beta decay (MeV) for intermediate ones [13–17] and at LHC through same-sign dileptons for heavy ones (100 GeV or above) [14, 18–26]. Furthermore, in the mass range of GeV to 100 GeV, the sterile neutrino would be metastable or long-lived at the detector scale, and can be probed at beam-dump types of experiments [27–39] (see also a review [40]), Very recently, the searches for sterile neutrino at the LHC started to develop actively as part of the long-lived particles searches covering the GeV scale [3, 41–57].

In this work, we focus on sterile neutrino production from W boson decay, which leads to a signature of a prompt lepton and a displaced but non-isolated lepton. A central challenge for new phenomenological studies on long-lived particles at the LHC is how to estimate the corresponding background. We overcome, at least partially, this challenge by extracting background behavior information from two very similar control regions measured and validated by an experimental search targeting different signatures at CMS [58]. We show the LHC sensitivity would be improved significantly in the regime of sterile neutrino mass around 1-20 GeV with a mixing angle squared between 10^{-8} to 10^{-3} .

The paper is organized as follows. In Sec. II, we provide a brief review of the seesaw models. In Sec. III, we discuss the properties of the sterile neutrino relevant for this study. In Sec. IV, we present the proposed analysis with the corresponding background estimation and the resulting for model parameter coverage. Finally, we conclude and discuss future directions in Sec. V.

II. STERILE NEUTRINO MODELS

In this section, we briefly review a few classes of seesaw models to motivate the parameter space we focus on. We begin with the original seesaw models [59–63] with the interaction Lagrangian of the new sterile neutrino sector

$$\Delta\mathcal{L}_\nu = -\lambda_\nu \bar{L}\tilde{H}N - \frac{m_N}{2}\bar{N}^c N + h.c., \quad (1)$$

where $\tilde{H} = i\sigma_2 H^*$. The mass matrix in the flavor basis $\{\nu_L, N^c\}$ is

$$M_\nu = \begin{pmatrix} 0 & m_D \\ m_D & m_N \end{pmatrix}, \quad (2)$$

where $m_D = \lambda_\nu v/\sqrt{2}$ with the vacuum expectation value of the Higgs field $v = 246$ GeV. The mass of light and heavy neutrino are

$$m_\nu \equiv m_1 \simeq \frac{m_D^2}{m_N}, \quad m_2 \simeq m_N + \frac{m_D^2}{m_N} \simeq m_N \quad (3)$$

respectively, in the heavy Majorana mass limit. The mixing angle is $\sin\theta = m_D/m_N$, which yields a relation between the mixing angle, light (active) neutrino mass and heavy neutrino mass:

$$\sin^2\theta \simeq \frac{m_\nu}{m_N}. \quad (4)$$

As we shall see later, the mixing angle controls the phenomenology of the searches for the sterile neutrino N . Beyond the original (and the most basic) seesaw model, a number of extensions and variations have been proposed, with new parameters and deviations beyond the simple relation shown in Eq. 4. We mention two such examples, namely, inverse seesaw model [64, 65] or linear seesaw model [66–68]. These variations of seesaw models can be parameterized similarly, and they are more accessible (and testable) with a larger mixing angle while capable of reproducing the light neutrino mass. The phenomenology is controlled by the same set of phenomenologically relevant parameters $\sin \theta$ and m_N but with a different relation to Lagrangian parameters. In inverse seesaw, we have

$$\sin^2 \theta = \frac{m_\nu}{\mu} \quad (\text{inverse seesaw}), \quad (5)$$

where μ is a free parameter with the relation $m_\nu = \mu \left(\frac{m_D}{m_N} \right)^2$. Here m_N becomes a Dirac mass term of new sterile neutrinos and μ is the Majorana mass of one of the new species. For linear seesaw, the relation is

$$\sin \theta = \frac{m_\nu}{m_\psi} \quad (\text{linear seesaw}), \quad (6)$$

where m_ψ is an additional Dirac mass term small than m_N , and its presence will violate the lepton number. With the additional parameters introduced, we can attribute neutrino mass to these new parameters. Thereafter, we only focus on $\sin \theta$ and m_N which are both free parameters.

In the later sections, we will constrain the mixing angle $\sin \theta$ as a function of sterile neutrino mass m_N with experimental studies. To simplify this discussion and focus on demonstrating our strategy, we will make the simple assumption that all three generations of the active neutrinos mix with N equally. In the context of more general seesaw models, making this assumption does not commit us to a particular neutrino mass hierarchy. The collider signal studied in this paper mainly rely on final states with electrons and muons, while the mixing with τ neutrino enters the decay width of the sterile neutrino if $m_N > m_\tau$. If we relax the assumption of universal mixing, the reach can be obtained from our result by rescaling relevant rates.

In the basic seesaw model, the mixing angle is not a free parameter for a particular sterile neutrino mass. It is fixed to be around

$$\sin^2 \theta \simeq 10^{-12} \left(\frac{m_\nu}{0.01 \text{ eV}} \right) \left(\frac{10 \text{ GeV}}{m_N} \right), \quad (7)$$

which is very difficult to be probed at the colliders. Still, in the context of more extended models, larger mixing angle is allowed. It is these non-minimal models which would be the main target for LHC searches.

III. STERILE NEUTRINO PROPERTIES

In this section, we discuss the features and properties of sterile neutrino from the extended seesaw models, with mixing angle $\sin\theta$ and mass m_N as free parameters. Due to the mixing between SM neutrino ν and sterile neutrino N , the relevant interactions are

$$\mathcal{L} = \frac{g \sin\theta}{\sqrt{2}} (W_\mu \bar{\ell}_L \gamma^\mu N + h.c.) - \frac{g \cos\theta \sin\theta}{2 \cos\theta_w} Z_\mu (\bar{\nu}_L \gamma^\mu N + \bar{N} \gamma^\mu \nu_L) + \frac{g \sin^2\theta}{2 \cos\theta_w} Z_\mu \bar{N} \gamma^\mu P_L N, \quad (8)$$

where θ_w is the weak mixing angle.

In a large region of parameter spaces of interests, the right-handed neutrino has a macroscopic lifetime

$$c\tau \simeq 12 \text{ km} \times \left(\frac{10^{-12}}{\sin^2\theta} \right) \left(\frac{10 \text{ GeV}}{m_N} \right)^5, \quad (9)$$

with the details of partial decay widths following [43, 69], see also [70, 71]. The reference mixing angle squared 10^{-12} is chosen for SM neutrino mass to 0.01 eV in the basic seesaw model. For an intermediate value of the mixing angle squared 10^{-6} , a 10 GeV sterile neutrino will still be long-lived at collider level with a proper lifetime of 12 mm. In Fig. 1, we show the partial widths, branching ratios and lifetime for heavy sterile neutrino N decay, with the assumption mixing angles between the three SM flavor neutrino are democratic $\sin\theta_{\nu_e N} = \sin\theta_{\nu_\mu N} = \sin\theta_{\nu_\tau N}$.

At colliders, the production of the sterile neutrino is the same as SM neutrinos, with additional suppression from mixing angle and kinematics. The production through the on-shell W boson is of particular interest here, given that the associated charge leptons can be used to trigger the signal processes. The long-lived sterile neutrino can then be analyzed without trigger penalties. The expected total number of sterile neutrino at the HL-LHC for one generation of democratic sterile neutrino is approximately

$$\mathcal{L} \times \sigma(pp \rightarrow W^\pm) \text{Br}(W^\pm \rightarrow \ell^\pm N) \simeq 1.8 \times 10^5 \left(\frac{\sin^2\theta}{10^{-6}} \right), \quad (10)$$

where $\mathcal{L} = 3000 \text{ fb}^{-1}$ is the integrated luminosity at the HL-LHC.

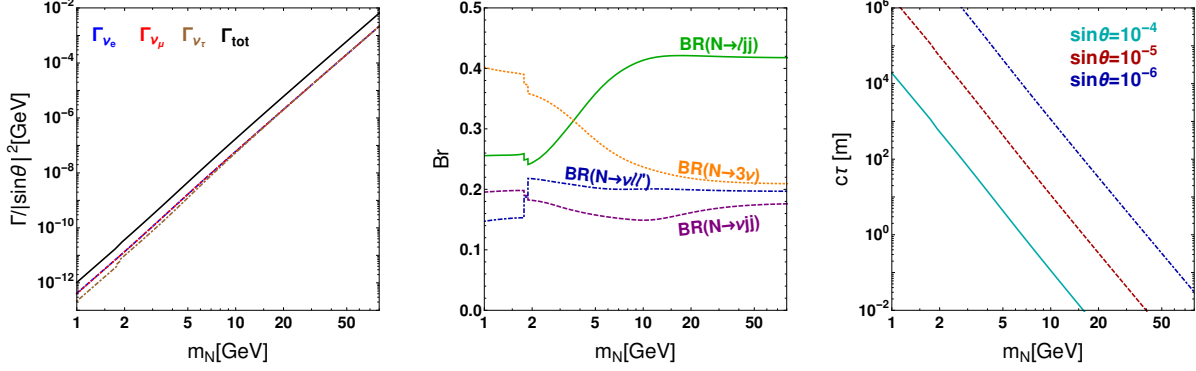


FIG. 1. The decay partial widths, branching ratios and lifetime for heavy sterile neutrino N , under a democratic mixing assumption $\sin\theta_{\nu_e N} = \sin\theta_{\nu_\mu N} = \sin\theta_{\nu_\tau N} = \sin\theta$. In the left panel, we show the partial decay width from mixing with ν_e , ν_μ , ν_τ and total decay width respectively. In the middle panel, we show the branching ratios to leptonic channels $\nu\ell\ell'$, $\nu\nu\nu$ and semi-leptonic channels ℓjj and νjj . In the right panel, we show the lifetime as a function of m_N with benchmark mixing angle $\sin\theta = 10^{-4}$, 10^{-5} and 10^{-6} respectively.

It is worth noting that the existence of two other SM venues for heavy sterile neutrino production, namely the Z boson decay and the Higgs boson decay. These two channels will become competitive if displaced-track triggers becoming available [72], which can provide a similar amount of sterile neutrino in addition to the W boson decay. Furthermore, the Higgs channel has two exciting features, namely Higgs specific trigger options and large branching fractions. There are many sub-leading Higgs production channels which can be triggered on, especially the vector boson fusion channel and weak boson associated production channel. Although the Higgs boson production rate is three to four orders of magnitude smaller than the W and Z boson, the branching fraction of the Higgs boson to $\nu + N$ can be five orders of magnitude larger, given its small total width. In this study, we do not include these channels and save these interesting new production modes for future studies in association with displaced triggers.

On the top panel of Fig. 2, we show the transverse momentum and pseudo-rapidity p_T^N - η_N distribution for sterile neutrino N from W production $pp \rightarrow W \rightarrow \ell N$. The process is generated by MadGraph5_aMC@NLO [73], and the parton shower is performed by Pythia8 [74, 75]. The η distribution of N is symmetric and dominantly within the range between $[-4, 4]$. Moreover, its transverse momentum p_T^N peaks around $30 \sim 40$ GeV, which

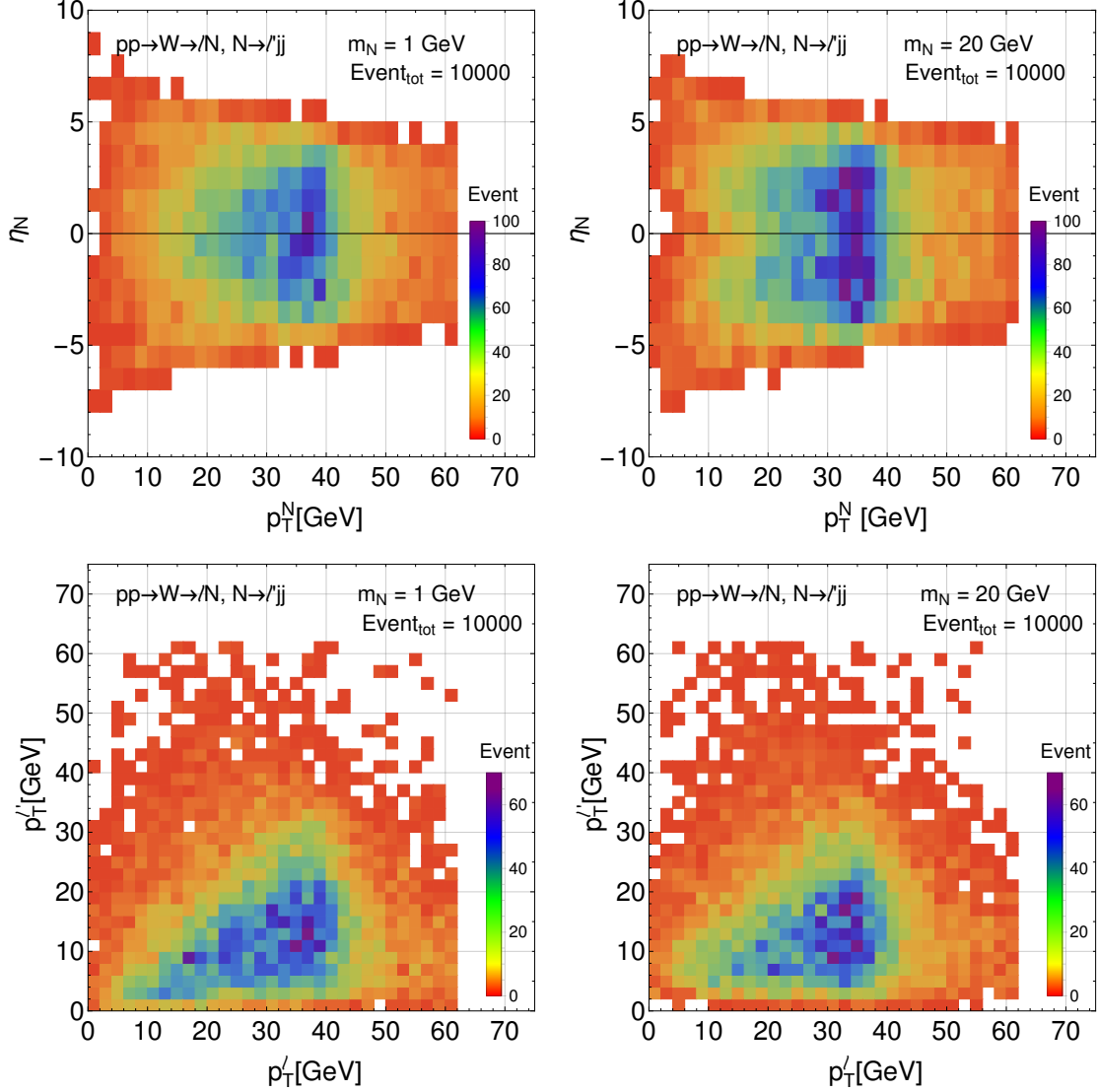


FIG. 2. Kinematics of the signals from the process $pp \rightarrow W \rightarrow \ell N$ with subsequent decay $N \rightarrow \ell' qq'$. *Top panel:* the transverse momentum p_T^N versus the pseudo-rapidity η_N of the sterile neutrino at the 13 TeV LHC. *Bottom panel:* the transverse momentum distribution of prompt lepton ℓ and the displaced lepton ℓ' . For the distributions, we have used mass $m_N = 1$ GeV and 20 GeV shown in the left panels and right panels, respectively. The total number of events is 10000, which corresponds to $\sin^2 \theta = 5.5 \times 10^{-8}$ at integrated luminosity $\mathcal{L} = 3 \text{ ab}^{-1}$ for HL-LHC.

is dictated by the maximum momentum it can obtain from W decay in the center of mass frame, $(m_W^2 + m_N^2) / (2m_W)$. For the events with p_T^N larger than this value, the initial state radiation provides additional transverse momentum of the W boson system. In the bottom panel of Fig. 2, we show the p_T distribution for both the prompt lepton ℓ from W decay

and displaced lepton ℓ' from N decay. The distribution of prompt lepton p_T^ℓ is similar to that of p_T^N , with the difference that the maximum momentum in center of mass frame becomes $(m_W^2 - m_N^2) / (2m_W)$. The displaced lepton transverse momentum, $p_T^{\ell'}$, is dominantly distributed within [5, 20] GeV, because the other two particles in the N decay take away approximately two thirds of the available energy.

IV. NEW SEARCHES STRATEGY FOR STERILE NEUTRINOS

There are many challenges to overcome to reach good sensitivities in the search for sterile neutrinos at the LHC. A major challenge is how to achieve a good signal selection efficiency with effective background suppression. Typical neutrino mass models point to tiny couplings between the sterile neutrino and the SM electroweak gauge bosons, leading to displaced decays of the sterile neutrinos. Therefore, a very effective strategy is necessary to pick out these displaced events at the LHC. Another aspect is triggering. The sterile neutrino can be produced in electroweak processes, which typically give rise to soft objects. At the same time, due to the low signal rates, the triggering needs to be as efficient as possible.

We consider the process of $pp \rightarrow W \rightarrow N\ell$, with a subsequent displaced decay of the sterile neutrino $N \rightarrow \ell'jj$. Since the prompt lepton ℓ is hard, one can in principal trigger the event using single lepton trigger. According to CMS Phase-2 upgrade of the level-1 trigger [76], the trigger thresholds (with track trigger) on a single lepton is $p_T > 27$ (31) GeV for isolated (non-isolated) e , and 18 GeV for μ . As shown in the prompt lepton p_T distribution in Fig. 2, the signal events will be reduced substantially by the single lepton trigger. Therefore, we consider double lepton trigger with the leading lepton $p_T > 19$ GeV and the sub-leading lepton with $p_T > 10.5$ GeV, also benefits from the track trigger [76]. In reality, the combination of triggers will be used in the experiment. Therefore, it is expected that the trigger efficiency will be better than using a single trigger category. Therefore, our approach on the triggering in this study is conservative.

For the off-line signal selection, the major advantage is the presence of a bundle of tracks with large (transverse) impact parameter, d_0 . We denote the decay position of sterile neutrino N as (x, y, z) with the production point being the origin, and the momentum of a daughter particle from N decay in x-y plane is denoted as (p_x, p_y) . We can define the

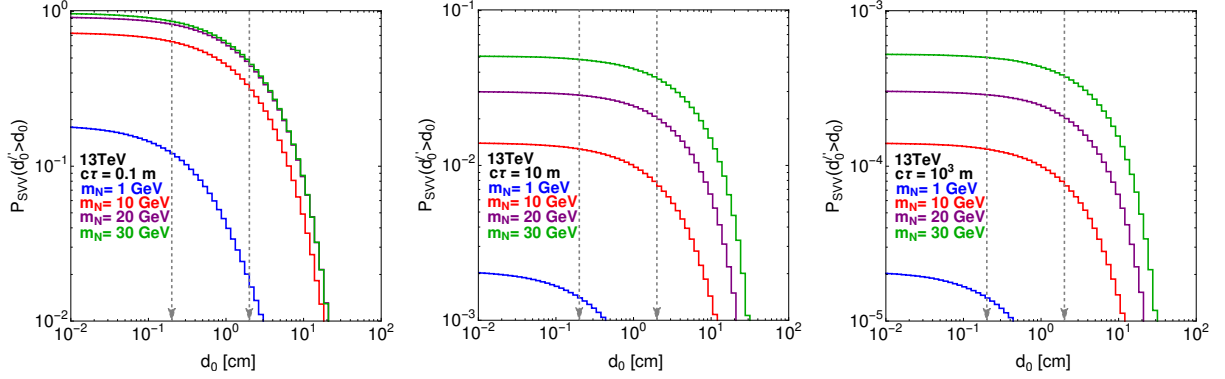


FIG. 3. The survival probability $P_{\text{SVV}}(d_{\ell'}^{\ell} > d_0)$ for the lepton ℓ' from the sterile neutrino decay $N \rightarrow \ell' j j$, as a function of the minimal d_0 cut. From left to right, the proper lifetime of sterile neutrino $c\tau$ are set as 0.1, 10 and 1000 meters, respectively. The two gray dashed arrows show $d_0 = 0.2$ cm and $d_0 = 2$ cm, which correspond to our benchmark selection cut.

transverse impact parameter d_0 as¹

$$d_0 = \sqrt{x^2 + y^2 - \frac{(xp_x + yp_y)^2}{p_x^2 + p_y^2}}. \quad (11)$$

We require the sterile neutrino N to decay within the detector region $r < 0.5$ m and $|z| < 1.2$ m, where r is the radial distance to the beam line. These numbers are chosen to guarantee that the lepton from the decay of the sterile neutrino would pass at least four Outer Tracker layers in either central or forward region, based on the Phase-2 upgrade of the CMS tracker [77]. Moreover, each layer of Outer Tracker consists of two closely spaced silicon sensors, which are called p_T modules to reject the low p_T tracks. The threshold is about 2 GeV which is easy to satisfy for our signal, based on the p_T distribution of displaced lepton in Fig. 2 and in particular for the events passing our trigger selection. The silicon sensors have a good granularity to provide sufficient spatial resolution and the module has a p_T resolution of 5%. If the electromagnetism calorimetry also has an excellent pointing resolution, using one layer of the Outer Tracker could be good enough to identify the direction of the track and measure the p_T , the detector region can be enlarged to $r \lesssim 1$ m and $|z| \lesssim 2.5$ m. In this case, the volume of the detector is increased by a factor of 8, leading to a significant

¹ For simplicity, we ignore the bending of tracks in this study as the displaced leptons p_T is sufficiently large. Furthermore, the hard prompt lepton enable us to reconstruct the three-dimensional position of the primary vertex, additional requirement on the three-dimensional impact parameter can compensate this simplification and improve our results.

improvement of the reach. We leave this possibility to future experimental studies and keep our conservative requirement on the number of track layers to hit.

The signal is selected first by imposing the dilepton trigger with $|\eta_\ell| < 2.5$ and requiring the long-lived sterile neutrino N decays in the detector region $r < 0.5$ m and $|z| < 1.2$ m. We further require the displaced lepton in the event has a large transverse impact parameter $d_0^{\ell'} > d_0$. The survival possibility is the number of such events divided by the total signal events, which we denoted as P_{SVV} . We plot its distributions with different sterile neutrino mass m_N and proper lifetime $c\tau$ in Fig. 3. For a given proper lifetime, a smaller sterile neutrino mass m_N leads to a lower P_{SVV} . This is a result of the kinematics of the resonance decay. Smaller sterile neutrino mass has larger boost factor, reducing the decay probability of sterile neutrino inside the detector region and reducing the displaced lepton opening angles to give a smaller d_0 . For $c\tau = 0.1$ m, a significant portion of the sterile neutrino produced decay within the region of the detector we focused on. A notable exception is when the sterile neutrino is light. For example, the P_{SVV} is significantly smaller for $m_N = 1$ GeV than other masses since it would often decay outside the region due to the large boost. For $c\tau = 10$ m and 10^3 m, the survival probabilities for different m_N s are roughly proportional to m_N^{-1} due to the boost factor of N . For the same m_N , the probabilities of $c\tau = 10$ m and 10^3 m differ by a factor of 100, exactly proportional to $(c\tau)^{-1}$ as expected in the long lifetime limit. In summary, the survival probabilities in Fig. 3 are mostly determined by the probability for N decay inside the required region, which is proportional to distance parameter d_N^{-1} . Here, $d_N = c\tau\gamma_N\beta_N$ is the expected decay distance in the laboratory frame, where γ_N is the boost factor and β_N is the velocity of N .

The signal contains one prompt lepton and another displaced lepton. The estimation of the Standard Model (SM) background of a newer search for a long-lived particle is always a challenge at the LHC. Fortunately, many important features of the corresponding background have been effectively explored as the control regions in a search for displaced electron plus muon search at CMS [58]. This search was performed with 2.6 fb^{-1} of 13 TeV LHC data, and it looks for a pair of displaced isolated leptons with different flavors with minimum p_T of 38 GeV each, targeting signals from pair produced top squarks decaying leptonically. The control regions (CR) of the background for this search helps to identify the dominant background of our new signals for long-lived sterile neutrinos. Specifically, the CR-III and CR-IV of this analysis requires one prompt lepton with transverse impact

parameter *smaller* than 200 μm and a displaced lepton with transverse impact parameter *greater* than 100 μm . The CR-III looks for a heavy flavor jet plus a displaced electron and CR-IV looks for a heavy flavor jet plus a displaced muon. CR-III is triggered by a singlet electron trigger (with electron $p_T > 20$ GeV), while CR-IV is triggered by a muon plus jet trigger (with a muon $p_T > 10$ GeV and jet $p_T > 12$ GeV), both with low p_T threshold for the leptons [78].

The CMS study [58] shows that the displaced leptons dominantly come from the heavy flavor QCD events (HF), because B and D mesons have sizable lifetimes. They simulate the HF+ ℓ data, requiring one tagged b-jet and one displaced lepton from the other heavy flavor quark. They further use a data driven method with the $e + \mu$ data and obtain the d_0 spectrum for one lepton while requiring the other lepton being prompt ($d_0 < 200$ μm). In figure 3, they show the agreement in the d_0 distribution between HF+ ℓ and $e + \mu$ data ². As a result, the detailed studies of these control regions in Ref. [58] confirm the following crucial fact about the displaced background distribution. First of all, the displaced leptons are dominantly from heavy flavor jets (b-jets) by using the “tag and probe” method where the jet recoil against the displaced lepton is tagged as a b-jet. The subleading background is from $t\bar{t}$ which is smaller by more than one order of magnitude, agreeing well with our simulation. Furthermore, for the displaced lepton, the (normalized) differential distribution as a function of the transverse impact parameter is shown to be the same for *isolated* and *non-isolated* leptons.

In Fig. 2 of Ref. [58], the background events are dominated by heavy flavor. Summing up all the d_0 bins, the corresponding cross-sections are 16.6 pb for HF+ e and 259 pb for HF+ μ respectively. We denote them as $\sigma_{\text{HF}+e}^{\text{CMS}}$ and $\sigma_{\text{HF}+\mu}^{\text{CMS}}$ respectively. The HF+ μ background is much larger than HF+ e background because the muon plus jet trigger requires a softer lepton than the single electron trigger. We used these results to validate our own simulation. In particular, we generated $b\bar{b}$ events and require e or μ to show up in the event after hadron fragmentation using Pythia8. We apply the CR-III and CR-IV triggers separately and further require at least one b-tagged jet. For HF+ e , the isolation requirement for the

² However, there are some differences between the CR-III (IV) data and the HF+ ℓ data. First, the CR-III and CR-IV do require one prompt and one displaced leptons, and the leptons satisfy the preselection for leptons. Moreover, the heavy flavor jet is not required for CR-III and IV, which is required for HF+ ℓ control data only. Second, HF+ ℓ control data only requires one displaced lepton from the heavy flavor quark. Thus, HF+ ℓ control data is not the same as CR-III and IV data, and is used to provide the d_0 shape information only.

electron is $\Delta R_e < 0.3$ and the additional p_T sum within the isolation cone should be less than 3.5% (6.5%) of the electron's p_T in the barrel (endcap) region. For HF+ μ , the isolation requirement for the muon is $\Delta R_\mu < 0.4$ and the additional p_T sum within the isolation cone should be less than 15% of the muon p_T . We implement these requirements by modifying the `Delphes3` [79]. For b-tagging efficiency, we have used the working point in [80], with 55% tagging efficiency for a b-jet with $p_T > 30$ GeV and $|\eta| < 2.4$. We found the corresponding cross-sections to be 21.9 pb and 241.2 pb for HF+ e and HF+ μ backgrounds, which are consistent with our extraction from Ref. [58]. We denote them as $\sigma_{bb(e)}^{\text{icut}}$ and $\sigma_{bb(\mu)}^{\text{icut}}$ which are the cross-sections after cuts with isolation requirement on leptons, denoted as ‘‘icut’’ in the superscript. Such consistency provides confidence when we calculate the background to our new search³.

The displaced lepton in the signal is often *non-isolated*. Therefore, a major background comes from events with a displaced *non-isolated* lepton from heavy flavor jets and a prompt lepton. Consequently, the leading backgrounds for our signal could be $W + b\bar{b}$ with W decaying leptonically, and $t\bar{t}$ with one of the top quarks decay leptonically. The number of the background can be calculated as

$$N_{\text{bkg}} = \frac{\sigma_{\text{HF}+e}^{\text{CMS}} + \sigma_{\text{HF}+\mu}^{\text{CMS}}}{\sigma_{bb(e)}^{\text{icut}} + \sigma_{bb(\mu)}^{\text{icut}}} \left(\sigma_{W+b\bar{b}, W \rightarrow \ell\nu}^{\text{ncut}} \times \epsilon_{\text{opt}}^{W+b\bar{b}} + \sigma_{t\bar{t} \rightarrow b\bar{b}+\ell+X}^{\text{ncut}} \times \epsilon_{\text{opt}}^{t\bar{t}} \right) \times \mathcal{L}_{\text{HL-LHC}}, \quad (12)$$

where the ‘‘ncut’’ in the upper script means requiring jets with $p_T^j > 20$ GeV while having one *non-isolated* lepton in the final states. In the event generation, we require b quark $p_T^b > 30$ GeV at parton level to ensure an energetic *non-isolated* lepton from its hadronic fragmentation. Otherwise, it is difficult to pass the lepton p_T cut. The lepton ℓ represent both e and μ . Further optimization selections are applied to both the signal and background, whose selection efficiencies are denoted as ϵ_{opt} in Eq. 12. The cross-sections $\sigma_{t\bar{t} \rightarrow b\bar{b}+\ell+X}^{\text{ncut}}$ and $\sigma_{W+b\bar{b}, W \rightarrow \ell\nu}^{\text{ncut}}$ are found to be 136 pb and 3.8 pb respectively, after applying the ‘‘ncut’’.

To further reduce the SM background, especially those from the $t\bar{t}$ process, additional cuts on the hadronic activities can help. In Fig. 4, we show the normalized distribution for the number of b-jets with $p_T^b > 30$ GeV denoted as N_b^{30} , the number of jets with $p_T^j > 20$ GeV denoted as N_j^{20} , the number of jets with $p_T^j > 50$ GeV denoted as N_j^{50} and H_T^{vis} , where H_T^{vis} is the scalar sum of p_T for all visible objects, including hadronic jets and leptons. We

³ We thank Bingxuan Liu on the analysis of Ref. [58] for clarifying the details of the control region in the analysis and confirming our scaling method.

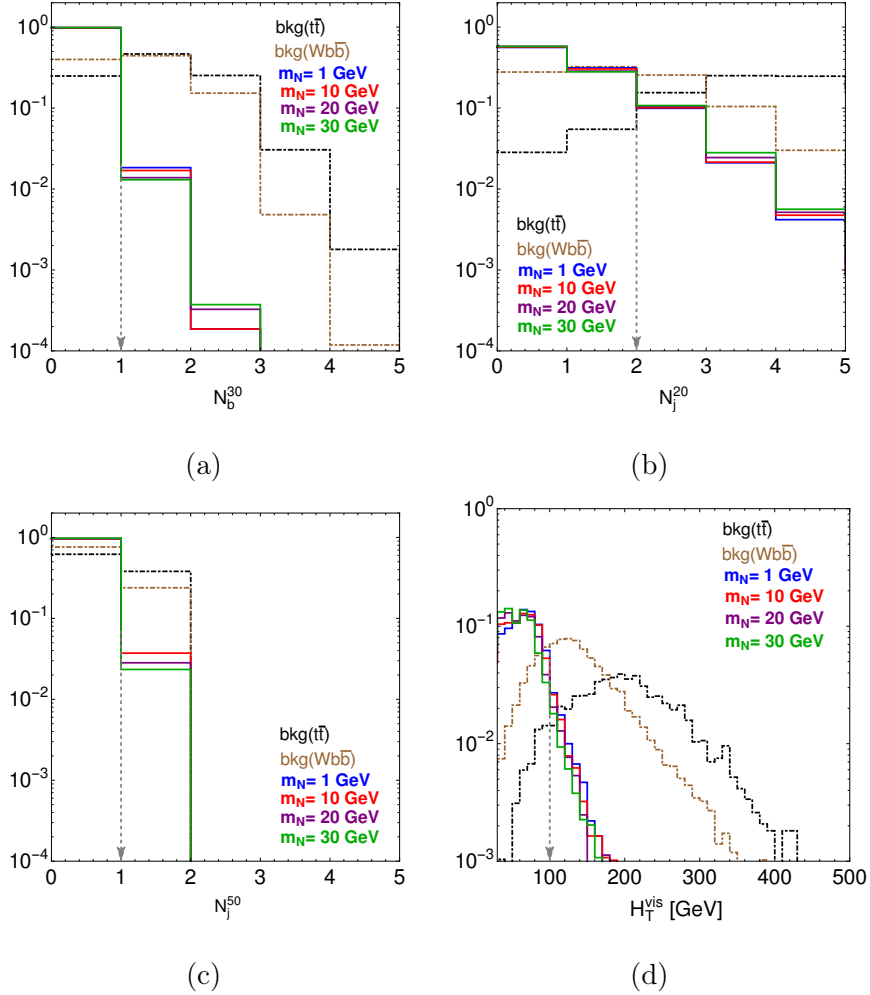


FIG. 4. The normalized distribution for the number of b-jets with $p_T^b > 30$ GeV denoted as N_b^{30} , the number of jets with $p_T^j > 20$ GeV denoted as N_j^{20} , the number of jets with $p_T^j > 50$ GeV denoted as N_j^{50} and H_T^{vis} , where H_T^{vis} is the scalar sum of p_T for all visible objects, including hadronic jets and leptons. The two SM backgrounds $t\bar{t} \rightarrow b\bar{b} + \ell + X$ and $W + b\bar{b}$, $W \rightarrow \ell\nu$ are dot-dashed lines with black and brown color respectively. The signals are solid lines with blue, red, purple and green colors for increasing m_N . The dashed gray lines with arrow indicates the optimization cuts that the events to its left are retained, namely $N_b^{30} = 0$, $N_j^{20} < 2$, $N_j^{50} = 0$ and $H_T^{vis} < 100$ GeV. The above cuts have been applied after its distribution have been shown in figure (a), (b), (c), and (d).

choose the optimization condition $N_b^{30} = 0$, $N_j^{20} < 2$, $N_j^{50} = 0$ and $H_T^{vis} < 100$ GeV to suppress the SM background without a significant reduction of the signal events. In Fig. 4, the above cuts have been applied after its distribution have been shown in sub-figures (a), (b), (c), and (d). We have included the jet matching in the background simulation. For $N_{j,b}$

and H_T observables, the $t\bar{t}$ background has slight differences between the results with and without jet matching. In addition, the $W + b\bar{b}$ backgrounds have even smaller difference than $t\bar{t}$ background. We also include the efficiency information for the dilepton trigger requirement $p_T^{\ell_1} > 19$ GeV and $p_T^{\ell_2} > 10.5$ GeV. The effects of various selection cuts and the total efficiencies are given in Table. I.

| Efficiency | σ^{ncut} (pb) | $N_b^{30} = 0$ | $N_j^{20} < 2$ | $N_j^{50} = 0$ | $H_T^{\text{vis}} < 100$ GeV | $p_T^{\ell_1} > 19\text{GeV}$ | $p_T^{\ell_2} > 10.5\text{GeV}$ | ϵ_{opt} |
|--|-----------------------------|----------------|----------------|----------------|------------------------------|-------------------------------|---------------------------------|-------------------------|
| $t\bar{t} \rightarrow b\bar{b} + \ell + X$ | 136 | 0.25 | 0.08 | 0.62 | 0.43 | 0.055 | 0.42 | 1.2×10^{-4} |
| $W + b\bar{b}, W \rightarrow \ell\nu$ | 3.8 | 0.40 | 0.60 | 0.76 | 0.40 | 0.27 | 0.29 | 5.7×10^{-3} |

TABLE I. The selection efficiency for the two dominant SM backgrounds $t\bar{t}$ with only one top quark decaying leptonically and $W + b\bar{b}$ with W decaying leptonically. The efficiencies reported in the table are the additional suppression with respect to all the previous cuts, and ϵ_{opt} is the total efficiency given by the product of all the cut efficiencies.

After combining all the cuts and optimizations, the backgrounds from $t\bar{t}$ and $W + b\bar{b}$ are 0.017 pb and 0.022 pb respectively, which are comparable in size. Multiplying by the integrated luminosity 3000 fb^{-1} from HL-LHC, the corresponding number of SM backgrounds are about 51000 and 65100 respectively. We assume for the SM background, the d_0 distribution for the lepton does not depend strongly on the p_T of the lepton and other optimization cuts on jets. Together with the fact that *isolated* and *non-isolated* lepton has the same distribution, we can use the normalized differential d_0 distribution from Ref. [58] to determine the background.

In Fig. 5, we plot the total number of SM background after applying $d_0^\ell > d_0$ with all the cuts and optimizations applied. Since the differential distribution of d_0 from CMS study [58] stops at 0.5 cm, we linearly extrapolate their data beyond that for the case of a larger d_0 cut of 2 cm. Moreover, their last bin, ([0.2, 0.5] cm), contains the overflow entries, thus our extrapolation is reasonably conservative. The SM background decreases linearly with d_0 cut in Fig. 5. After comparing with the d_0 accumulative distribution for signal in Fig. 3, we adopt two benchmarks for the displacement, requiring $d_0 > 0.2$ cm and 2 cm, respectively. From Fig. 5, the total number of background event is around 2000 for $d_0 > 0.2$ cm and 100 for $d_0 > 2$ cm. Despite the analysis of SM background above, it can also be estimated in a data-driven method similar to the CMS search. For instance, one can study the d_0

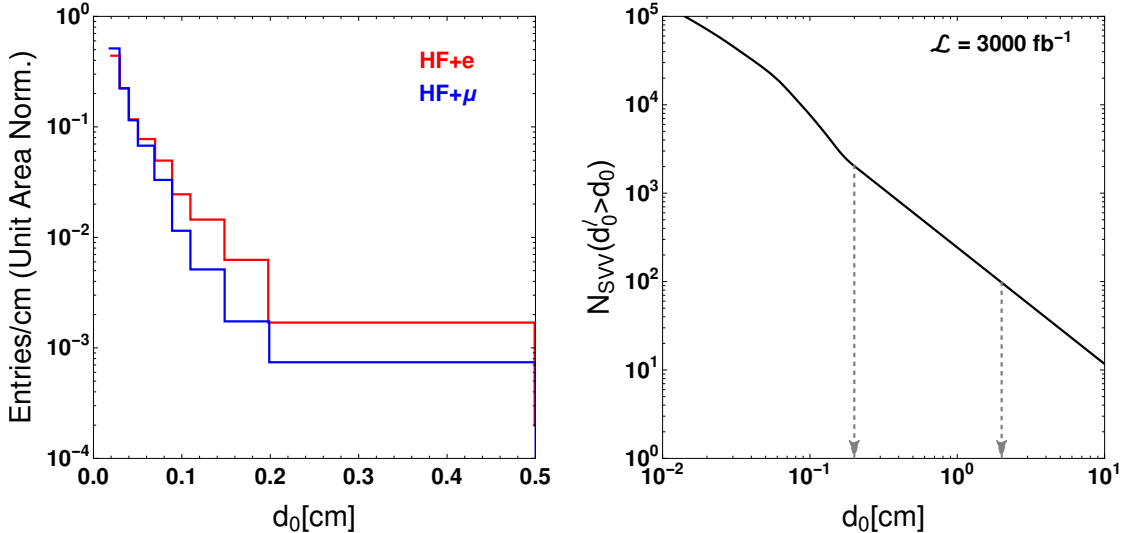


FIG. 5. *Left panel:* The normalized d_0 distribution for HF+ e and HF+ μ control regions from Ref. [58]. *Right panel:* The total number of SM background after applying minimal d_0 cut with all the trigger and selection cuts applied, denoted as $N_{\text{SVV}}(d_0^\ell > d_0)$. The two dashed gray lines with arrow indicates two of our benchmark minimal d_0 cuts of 0.2 cm and 2 cm selection.

distribution of the non-isolated leptons using the “tag and probe” method, same as what have done in the heavy flavor plus lepton control region. Furthermore, one can also study the invariant mass distribution of the non-isolated lepton (plus hadrons) system. Future studies could also include more exclusive decays of the sterile neutrino to reconstruct the mass and reject the background more efficiently. Moreover, heavy long-lived sterile neutrinos will also be time-delayed. These additional features can help define the control region in a more sophisticated manner and will certainly improve the sensitivity.

With the above background estimation, we derive the 95% C.L. sensitivity for sterile neutrino in red shaded region in Fig. 6, where the left and right panel are for $d_0 > 0.2$ cm and $d_0 > 2$ cm, respectively. In Ref. [58], the systematic uncertainties for different SM backgrounds vary from 5% to 10%. Therefore, we conservatively assume systematic uncertainty for SM backgrounds to be 10%. The corresponding sensitivity curves with the systematic uncertainty are plotted in dashed red lines in Fig. 6. In general, the upper edge of the sensitivity region corresponds to the shorter lifetime. It is driven by the lower cut on the transverse impact parameter d_0 and we see clear advantage for smaller cut on d_0 , even though the number of SM background is larger. On the other hand, the lower edge of the

red shaded region corresponds to the longer lifetime, which is insensitive to the d_0 cut.

In Fig. 6, we plot the leading constraints from CMS [81] and DELPHI [82]. The CMS collaboration [81] looks for heavy sterile neutrinos in events with three prompt charged leptons, while the DELPHI collaboration [82] looks for both short-lived and long-lived sterile neutrinos in hadronic Z decay events. We have combined these two constraints together and shown the exclusions in shaded gray region. For sterile neutrino mass smaller than 2 GeV, the more important constraints are from beam dump experiments, like NuTeV [34], CHARM [28, 32], BEBC [29], and FMMF [33]. Their constraints are also shaded in gray color. In Fig. 6, we also show the projected sensitivity from a proposed displaced vertex search at the LHC in dot-dashed curves [83] and various proposals for fix target or satellite detector experiments [37, 38, 52, 53, 84] in dashed curves. The LBNE collaboration [37] is a long-baseline neutrino experiment also named as DUNE, which measures the sterile neutrino and active neutrino mixing by comparing the neutral current events between the near and far detectors. The SHiP collaboration [38, 84] is a fixed target facility (proton beam dump) probing the mixing by the signature of displaced secondary vertex from sterile neutrino decay. The MATHUSLA collaboration [53] is a far detector proposal for the LHC and also measures the mixing with displaced sterile neutrino decay. The FASER [52] is another far detector proposal, but is placed in the forward region. Those future projections are plotted in dashed lines in the figure. It is clear that our more inclusive search allows us to explore parameter spaces of the sterile neutrino with lighter masses. Furthermore, when compared with other fixed target experiment and satellite detector experiments, our proposal covers new regions of sterile neutrinos whose lifetime is too short to have sufficient flux for these experiments. In the long run, if any discoveries were made, the regions overlapping with different searches and experiments will provide valuable information for the underlying new physics model.⁴

V. CONCLUSION AND OUTLOOK

In this paper, we study the signal of long-lived sterile neutrino N from W -boson decay, $W \rightarrow \ell N$, with the subsequent decay of $N \rightarrow \ell' jj$. The characteristic feature is a

⁴ A recent study [83] projected that with a prompt lepton trigger with associated hadronic displaced vertex at HL-LHC, and assuming zero background, could cover the regime of sterile neutrinos with mass between 10-20 GeV, complementing our search.

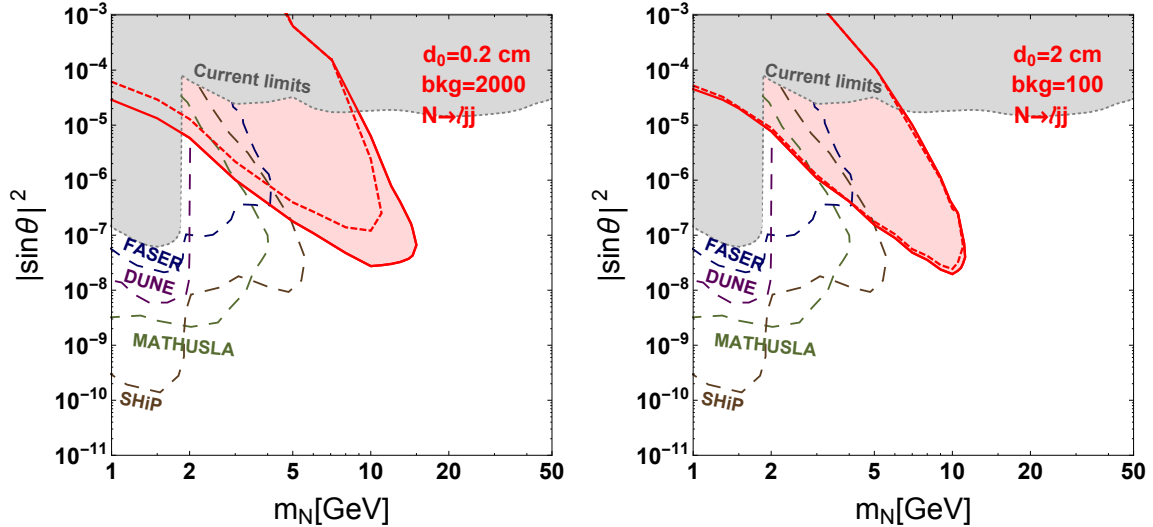


FIG. 6. The 95% C.L. reach for sterile neutrino from W gauge boson decay is plotted in the m_N - $\sin^2\theta$ plane with solid red lines. The dashed red lines have included 10% systematic uncertainty effect. The existing constraints are from CMS [81] and DELPHI [82] for mass larger than 1 GeV. While for mass smaller than 2 GeV, the stronger constraints are from beam dump experiments like NuTeV [34], CHARM [28, 32], BEBC [29], and FMMF [33]. The existing current limits are shaded in gray color and labeled as “Current limits”. The proposed sensitivity reaches for MATHUSLA [53], FASER [52], DUNE [37] and SHiP [38, 84] are shown in dashed curves.

hard prompt lepton with a displaced lepton with large transverse impact parameter d_0 . We neither reconstruct the displaced vertex nor cut on its invariant mass, therefore it can be sensitive for very low sterile neutrino mass. However, there is a crucial subtlety that with such small masses, the displaced lepton is usually *non-isolated* from the other two jets in the same N decay. To estimate the background, we have used the information from a search for displaced electron plus muon search at CMS [58] which studied relevant background in its control regions. It shows that for *non-isolated* lepton, those from heavy flavor quarks are the dominant SM background. Moreover, it demonstrates the important fact that the normalized d_0 differential distribution has the same shape for *isolated* and *non-isolated* leptons. Therefore, we can use their d_0 distribution for the *non-isolated* lepton from heavy flavor quark background. We recast their control region selection and found a good agreement with their observations. This ensures our background estimations are robust. After proposing the optimization cuts for the signal, we obtain the result for the sensitivity on

parameters for the sterile neutrino. Our results can explore the region with light m_N and relative large mixing angle, which is not covered by the displaced vertex searches at LHC, beam dump and far detectors experiments.

There are many new exciting opportunities at the LHC, such as displaced tracker triggers proposed to be implemented at low-level at CMS by Ref. [85]. This trigger can be handy as a general trigger for long-lived particles in a broad class of theories [86], especially for physics signals hard to be triggered on using traditional trigger. Although we have applied two lepton trigger in this study, adding the displaced tracker trigger into the trigger menu can effectively lower the p_T requirement on the leptons. Moreover, the Phase-2 upgrade of the tracker system of CMS contains the Outer Tracker layer which is consisted of two closely spaced silicon sensors. It effectively doubles the hits of the track; therefore one can lower the requirement on the number of penetrating layers, which can increase the volume of the long-lived particle decay. It has the potential to significantly increase the sensitivity but the detailed realization needs further studies. Moreover, for heavier sterile neutrinos above 10 GeV, the long-lived sterile neutrino are time-delayed with respect to the SM backgrounds. This feature can be further utilized for trigger and background suppression considerations [87].

Note added. While we were finalizing this paper, Ref. [55], [56] and [57] appeared on the arXiv studying similar topics. The main focus of Ref. [55] is looking for sterile neutrino decay to lepton plus pions, using displaced vertex associated with low p_T muon. And their mass coverage for sterile neutrino is from 5 GeV to 20 GeV. The second paper [56] studies long-lived sterile neutrino in displaced vertex searches and also using muon chambers to detect the muons from such vertex. It uses invariant mass cut and displacement cut to suppress the SM background. The third paper [57] requires displaced vertex reconstructed by two muons in the CMS muon detector.

Acknowledgements: We thank Felix Kling, Jared Evans and Bingxuan Liu for helpful discussion. JL acknowledges support by an Oehme Fellowship. ZL is supported in part by the NSF under Grant No. PHY1620074 and by the Maryland Center for Fundamental Physics. XPW is supported by the U.S. Department of Energy under Contract No. DE-AC02-06CH11357. LTW is supported by the DOE grant DE-SC0013642. ZL thanks the Aspen Center for Physics, which is supported by National Science Foundation grant PHY-

1607611.

-
- [1] **Super-Kamiokande** Collaboration, Y. Fukuda *et al.*, “Evidence for oscillation of atmospheric neutrinos,” *Phys. Rev. Lett.* **81** (1998) 1562–1567, [arXiv:hep-ex/9807003 \[hep-ex\]](#).
- [2] **Super-Kamiokande** Collaboration, Y. Fukuda *et al.*, “Measurement of the flux and zenith angle distribution of upward through going muons by Super-Kamiokande,” *Phys. Rev. Lett.* **82** (1999) 2644–2648, [arXiv:hep-ex/9812014 \[hep-ex\]](#).
- [3] **SNO** Collaboration, Q. R. Ahmad *et al.*, “Direct evidence for neutrino flavor transformation from neutral current interactions in the Sudbury Neutrino Observatory,” *Phys. Rev. Lett.* **89** (2002) 011301, [arXiv:nucl-ex/0204008 \[nucl-ex\]](#).
- [4] **KamLAND** Collaboration, K. Eguchi *et al.*, “First results from KamLAND: Evidence for reactor anti-neutrino disappearance,” *Phys. Rev. Lett.* **90** (2003) 021802, [arXiv:hep-ex/0212021 \[hep-ex\]](#).
- [5] **Particle Data Group** Collaboration, M. Tanabashi *et al.*, “Review of Particle Physics,” *Phys. Rev.* **D98** no. 3, (2018) 030001.
- [6] **Planck** Collaboration, N. Aghanim *et al.*, “Planck 2018 results. VI. Cosmological parameters,” [arXiv:1807.06209 \[astro-ph.CO\]](#).
- [7] J. Kopp, P. A. N. Machado, M. Maltoni, and T. Schwetz, “Sterile Neutrino Oscillations: The Global Picture,” *JHEP* **05** (2013) 050, [arXiv:1303.3011 \[hep-ph\]](#).
- [8] C. Giunti, “Light Sterile Neutrinos: Status and Perspectives,” *Nucl. Phys.* **B908** (2016) 336–353, [arXiv:1512.04758 \[hep-ph\]](#).
- [9] F. Capozzi, C. Giunti, M. Laveder, and A. Palazzo, “Joint short- and long-baseline constraints on light sterile neutrinos,” *Phys. Rev.* **D95** no. 3, (2017) 033006, [arXiv:1612.07764 \[hep-ph\]](#).
- [10] S. Gariazzo, C. Giunti, M. Laveder, and Y. F. Li, “Updated Global 3+1 Analysis of Short-BaseLine Neutrino Oscillations,” *JHEP* **06** (2017) 135, [arXiv:1703.00860 \[hep-ph\]](#).
- [11] M. Dentler, A. Hernandez-Cabezudo, J. Kopp, M. Maltoni, and T. Schwetz, “Sterile neutrinos or flux uncertainties? — Status of the reactor anti-neutrino anomaly,” *JHEP* **11** (2017) 099, [arXiv:1709.04294 \[hep-ph\]](#).

- [12] M. Dentler, A. Hernandez-Cabezudo, J. Kopp, P. A. N. Machado, M. Maltoni, I. Martinez-Soler, and T. Schwetz, “Updated Global Analysis of Neutrino Oscillations in the Presence of eV-Scale Sterile Neutrinos,” *JHEP* **08** (2018) 010, [arXiv:1803.10661 \[hep-ph\]](#).
- [13] P. Benes, A. Faessler, F. Simkovic, and S. Kovalenko, “Sterile neutrinos in neutrinoless double beta decay,” *Phys. Rev.* **D71** (2005) 077901, [arXiv:hep-ph/0501295 \[hep-ph\]](#).
- [14] A. Atre, T. Han, S. Pascoli, and B. Zhang, “The Search for Heavy Majorana Neutrinos,” *JHEP* **05** (2009) 030, [arXiv:0901.3589 \[hep-ph\]](#).
- [15] M. Blennow, E. Fernandez-Martinez, J. Lopez-Pavon, and J. Menendez, “Neutrinoless double beta decay in seesaw models,” *JHEP* **07** (2010) 096, [arXiv:1005.3240 \[hep-ph\]](#).
- [16] W. Rodejohann, “Neutrino-less Double Beta Decay and Particle Physics,” *Int. J. Mod. Phys.* **E20** (2011) 1833–1930, [arXiv:1106.1334 \[hep-ph\]](#).
- [17] J. Barea, J. Kotila, and F. Iachello, “Limits on sterile neutrino contributions to neutrinoless double beta decay,” *Phys. Rev.* **D92** (2015) 093001, [arXiv:1509.01925 \[hep-ph\]](#).
- [18] W.-Y. Keung and G. Senjanovic, “Majorana Neutrinos and the Production of the Right-handed Charged Gauge Boson,” *Phys. Rev. Lett.* **50** (1983) 1427.
- [19] T. Han and B. Zhang, “Signatures for Majorana neutrinos at hadron colliders,” *Phys. Rev. Lett.* **97** (2006) 171804, [arXiv:hep-ph/0604064 \[hep-ph\]](#).
- [20] F. del Aguila, J. A. Aguilar-Saavedra, and R. Pittau, “Heavy neutrino signals at large hadron colliders,” *JHEP* **10** (2007) 047, [arXiv:hep-ph/0703261 \[hep-ph\]](#).
- [21] D. Alva, T. Han, and R. Ruiz, “Heavy Majorana neutrinos from $W\gamma$ fusion at hadron colliders,” *JHEP* **02** (2015) 072, [arXiv:1411.7305 \[hep-ph\]](#).
- [22] C. Degrande, O. Mattelaer, R. Ruiz, and J. Turner, “Fully-Automated Precision Predictions for Heavy Neutrino Production Mechanisms at Hadron Colliders,” *Phys. Rev.* **D94** no. 5, (2016) 053002, [arXiv:1602.06957 \[hep-ph\]](#).
- [23] Y. Cai, T. Han, T. Li, and R. Ruiz, “Lepton Number Violation: Seesaw Models and Their Collider Tests,” *Front.in Phys.* **6** (2018) 40, [arXiv:1711.02180 \[hep-ph\]](#).
- [24] E. Accomando, L. Delle Rose, S. Moretti, E. Olaiya, and C. H. Shepherd-Themistocleous, “Novel SM-like Higgs decay into displaced heavy neutrino pairs in U(1)’ models,” *JHEP* **04** (2017) 081, [arXiv:1612.05977 \[hep-ph\]](#).
- [25] E. Accomando, L. Delle Rose, S. Moretti, E. Olaiya, and C. H. Shepherd-Themistocleous, “Extra Higgs boson and Z' as portals to signatures of heavy neutrinos at the LHC,” *JHEP* **02**

- (2018) 109, [arXiv:1708.03650 \[hep-ph\]](#).
- [26] G. Cvetič, A. Das, and J. Zamora-Saá, “Probing heavy neutrino oscillations in rare W boson decays,” [arXiv:1805.00070 \[hep-ph\]](#).
- [27] **NA3** Collaboration, J. Badier *et al.*, “Direct Photon Production From Pions and Protons at 200-GeV/c,” *Z. Phys.* **C31** (1986) 341.
- [28] **CHARM** Collaboration, F. Bergsma *et al.*, “A Search for Decays of Heavy Neutrinos in the Mass Range 0.5-GeV to 2.8-GeV,” *Phys. Lett.* **166B** (1986) 473–478.
- [29] **WA66** Collaboration, A. M. Cooper-Sarkar *et al.*, “Search for Heavy Neutrino Decays in the BEBC Beam Dump Experiment,” *Phys. Lett.* **160B** (1985) 207–211.
- [30] G. Bernardi *et al.*, “FURTHER LIMITS ON HEAVY NEUTRINO COUPLINGS,” *Phys. Lett.* **B203** (1988) 332–334.
- [31] S. A. Baranov *et al.*, “Search for heavy neutrinos at the IHEP-JINR neutrino detector,” *Phys. Lett.* **B302** (1993) 336–340.
- [32] **CHARM II** Collaboration, P. Vilain *et al.*, “Search for heavy isosinglet neutrinos,” *Phys. Lett.* **B343** (1995) 453–458. [*Phys. Lett.*B351,387(1995)].
- [33] **FMMF** Collaboration, E. Gallas *et al.*, “Search for neutral weakly interacting massive particles in the Fermilab Tevatron wide band neutrino beam,” *Phys. Rev.* **D52** (1995) 6–14.
- [34] **NuTeV, E815** Collaboration, A. Vaitaitis *et al.*, “Search for neutral heavy leptons in a high-energy neutrino beam,” *Phys. Rev. Lett.* **83** (1999) 4943–4946, [arXiv:hep-ex/9908011 \[hep-ex\]](#).
- [35] **NOMAD** Collaboration, P. Astier *et al.*, “Search for heavy neutrinos mixing with tau neutrinos,” *Phys. Lett.* **B506** (2001) 27–38, [arXiv:hep-ex/0101041 \[hep-ex\]](#).
- [36] J. Orloff, A. N. Rozanov, and C. Santoni, “Limits on the mixing of tau neutrino to heavy neutrinos,” *Phys. Lett.* **B550** (2002) 8–15, [arXiv:hep-ph/0208075 \[hep-ph\]](#).
- [37] **LBNE** Collaboration, C. Adams *et al.*, “The Long-Baseline Neutrino Experiment: Exploring Fundamental Symmetries of the Universe,” [arXiv:1307.7335 \[hep-ex\]](#).
- [38] **SHiP** Collaboration, M. Anelli *et al.*, “A facility to Search for Hidden Particles (SHiP) at the CERN SPS,” [arXiv:1504.04956 \[physics.ins-det\]](#).
- [39] M. Drewes, J. Hajer, J. Klaric, and G. Lanfranchi, “NA62 sensitivity to heavy neutral leptons in the low scale seesaw model,” *JHEP* **07** (2018) 105, [arXiv:1801.04207 \[hep-ph\]](#).
- [40] F. F. Deppisch, P. S. Bhupal Dev, and A. Pilaftsis, “Neutrinos and Collider Physics,” *New J.*

- Phys.* **17** no. 7, (2015) 075019, [arXiv:1502.06541 \[hep-ph\]](#).
- [41] M. L. Graesser, “Experimental Constraints on Higgs Boson Decays to TeV-scale Right-Handed Neutrinos,” [arXiv:0705.2190 \[hep-ph\]](#).
- [42] M. L. Graesser, “Broadening the Higgs boson with right-handed neutrinos and a higher dimension operator at the electroweak scale,” *Phys. Rev.* **D76** (2007) 075006, [arXiv:0704.0438 \[hep-ph\]](#).
- [43] J. C. Helo, M. Hirsch, and S. Kovalenko, “Heavy neutrino searches at the LHC with displaced vertices,” *Phys. Rev.* **D89** (2014) 073005, [arXiv:1312.2900 \[hep-ph\]](#). [Erratum: *Phys. Rev.* **D93**,no.9,099902(2016)].
- [44] A. Maiezza, M. Nemevšek, and F. Nesti, “Lepton Number Violation in Higgs Decay at LHC,” *Phys. Rev. Lett.* **115** (2015) 081802, [arXiv:1503.06834 \[hep-ph\]](#).
- [45] B. Batell, M. Pospelov, and B. Shuve, “Shedding Light on Neutrino Masses with Dark Forces,” *JHEP* **08** (2016) 052, [arXiv:1604.06099 \[hep-ph\]](#).
- [46] S. Antusch, E. Cazzato, and O. Fischer, “Displaced vertex searches for sterile neutrinos at future lepton colliders,” *JHEP* **12** (2016) 007, [arXiv:1604.02420 \[hep-ph\]](#).
- [47] M. Nemevsek, F. Nesti, and J. C. Vasquez, “Majorana Higgses at colliders,” *JHEP* **04** (2017) 114, [arXiv:1612.06840 \[hep-ph\]](#).
- [48] S. Antusch, E. Cazzato, and O. Fischer, “Sterile neutrino searches via displaced vertices at LHCb,” *Phys. Lett.* **B774** (2017) 114–118, [arXiv:1706.05990 \[hep-ph\]](#).
- [49] A. Caputo, P. Hernandez, J. Lopez-Pavon, and J. Salvado, “The seesaw portal in testable models of neutrino masses,” *JHEP* **06** (2017) 112, [arXiv:1704.08721 \[hep-ph\]](#).
- [50] G. Cottin, J. C. Helo, and M. Hirsch, “Searches for light sterile neutrinos with multitrack displaced vertices,” *Phys. Rev.* **D97** no. 5, (2018) 055025, [arXiv:1801.02734 \[hep-ph\]](#).
- [51] J. C. Helo, M. Hirsch, and Z. S. Wang, “Heavy neutral fermions at the high-luminosity LHC,” [arXiv:1803.02212 \[hep-ph\]](#).
- [52] F. Kling and S. Trojanowski, “Heavy Neutral Leptons at FASER,” *Phys. Rev.* **D97** no. 9, (2018) 095016, [arXiv:1801.08947 \[hep-ph\]](#).
- [53] D. Curtin *et al.*, “Long-Lived Particles at the Energy Frontier: The MATHUSLA Physics Case,” [arXiv:1806.07396 \[hep-ph\]](#).
- [54] A. Abada, N. Bernal, M. Losada, and X. Marcano, “Inclusive Displaced Vertex Searches for Heavy Neutral Leptons at the LHC,” *JHEP* **01** (2019) 093, [arXiv:1807.10024 \[hep-ph\]](#).

- [55] C. O. Dib, C. S. Kim, and S. Tapia Araya, “Search of light sterile neutrinos from W^\pm decays,” [arXiv:1903.04905 \[hep-ph\]](#).
- [56] M. Drewes and J. Hajer, “Heavy Neutrinos in displaced vertex searches at the LHC and HL-LHC,” [arXiv:1903.06100 \[hep-ph\]](#).
- [57] K. Bondarenko, A. Boyarsky, M. Ovchinnikov, O. Ruchayskiy, and L. Shchutska, “Probing new physics with displaced vertices: muon tracker at CMS,” [arXiv:1903.11918 \[hep-ph\]](#).
- [58] CMS Collaboration, “Search for displaced leptons in the e-mu channel,” Tech. Rep. CMS-PAS-EXO-16-022, CERN, Geneva, 2016. <http://cds.cern.ch/record/2205146>.
- [59] P. Minkowski, “ $\mu \rightarrow e\gamma$ at a Rate of One Out of 10^9 Muon Decays?,” *Phys. Lett.* **67B** (1977) 421–428.
- [60] M. Gell-Mann, P. Ramond, and R. Slansky, “Complex Spinors and Unified Theories,” *Conf. Proc.* **C790927** (1979) 315–321, [arXiv:1306.4669 \[hep-th\]](#).
- [61] R. N. Mohapatra and G. Senjanovic, “Neutrino Mass and Spontaneous Parity Nonconservation,” *Phys. Rev. Lett.* **44** (1980) 912. [,231(1979)].
- [62] T. Yanagida, “Horizontal Symmetry and Masses of Neutrinos,” *Prog. Theor. Phys.* **64** (1980) 1103.
- [63] J. Schechter and J. W. F. Valle, “Neutrino Masses in $SU(2) \times U(1)$ Theories,” *Phys. Rev.* **D22** (1980) 2227.
- [64] R. N. Mohapatra, “Mechanism for Understanding Small Neutrino Mass in Superstring Theories,” *Phys. Rev. Lett.* **56** (1986) 561–563.
- [65] R. N. Mohapatra and J. W. F. Valle, “Neutrino Mass and Baryon Number Nonconservation in Superstring Models,” *Phys. Rev.* **D34** (1986) 1642. [,235(1986)].
- [66] D. Wyler and L. Wolfenstein, “Massless Neutrinos in Left-Right Symmetric Models,” *Nucl. Phys.* **B218** (1983) 205–214.
- [67] E. K. Akhmedov, M. Lindner, E. Schnapka, and J. W. F. Valle, “Left-right symmetry breaking in NJL approach,” *Phys. Lett.* **B368** (1996) 270–280, [arXiv:hep-ph/9507275 \[hep-ph\]](#).
- [68] E. K. Akhmedov, M. Lindner, E. Schnapka, and J. W. F. Valle, “Dynamical left-right symmetry breaking,” *Phys. Rev.* **D53** (1996) 2752–2780, [arXiv:hep-ph/9509255 \[hep-ph\]](#).
- [69] J. C. Helo, S. Kovalenko, and I. Schmidt, “Sterile neutrinos in lepton number and lepton flavor violating decays,” *Nucl. Phys.* **B853** (2011) 80–104, [arXiv:1005.1607 \[hep-ph\]](#).

- [70] K. Bondarenko, A. Boyarsky, D. Gorbunov, and O. Ruchayskiy, “Phenomenology of GeV-scale Heavy Neutral Leptons,” *JHEP* **11** (2018) 032, [arXiv:1805.08567 \[hep-ph\]](#).
- [71] A. Das, N. Okada, S. Okada, and D. Raut, “Probing the seesaw mechanism at the 250 GeV ILC,” [arXiv:1812.11931 \[hep-ph\]](#).
- [72] Y. Gershtein, “CMS Hardware Track Trigger: New Opportunities for Long-Lived Particle Searches at the HL-LHC,” *Phys. Rev.* **D96** no. 3, (2017) 035027, [arXiv:1705.04321 \[hep-ph\]](#).
- [73] J. Alwall, R. Frederix, S. Frixione, V. Hirschi, F. Maltoni, O. Mattelaer, H. S. Shao, T. Stelzer, P. Torrielli, and M. Zaro, “The automated computation of tree-level and next-to-leading order differential cross sections, and their matching to parton shower simulations,” *JHEP* **07** (2014) 079, [arXiv:1405.0301 \[hep-ph\]](#).
- [74] T. Sjostrand, S. Mrenna, and P. Z. Skands, “PYTHIA 6.4 Physics and Manual,” *JHEP* **05** (2006) 026, [arXiv:hep-ph/0603175 \[hep-ph\]](#).
- [75] T. Sjostrand, S. Mrenna, and P. Z. Skands, “A Brief Introduction to PYTHIA 8.1,” *Comput. Phys. Commun.* **178** (2008) 852–867, [arXiv:0710.3820 \[hep-ph\]](#).
- [76] CMS Collaboration, “The Phase-2 Upgrade of the CMS L1 Trigger Interim Technical Design Report,” Tech. Rep. CERN-LHCC-2017-013. CMS-TDR-017, CERN, Geneva, Sep, 2017. <http://cds.cern.ch/record/2283192>. This is the CMS Interim TDR devoted to the upgrade of the CMS L1 trigger in view of the HL-LHC running, as approved by the LHCC.
- [77] CMS Collaboration, “The Phase-2 Upgrade of the CMS Tracker,” Tech. Rep. CERN-LHCC-2017-009. CMS-TDR-014, CERN, Geneva, Jun, 2017. <http://cds.cern.ch/record/2272264>.
- [78] CMS Collaboration, V. Khachatryan *et al.*, “The CMS trigger system,” *JINST* **12** no. 01, (2017) P01020, [arXiv:1609.02366 \[physics.ins-det\]](#).
- [79] DELPHES 3 Collaboration, J. de Favereau, C. Delaere, P. Demin, A. Giammanco, V. Lemaitre, A. Mertens, and M. Selvaggi, “DELPHES 3, A modular framework for fast simulation of a generic collider experiment,” *JHEP* **02** (2014) 057, [arXiv:1307.6346 \[hep-ex\]](#).
- [80] CMS Collaboration, S. Chatrchyan *et al.*, “Identification of b-quark jets with the CMS experiment,” *JINST* **8** (2013) P04013, [arXiv:1211.4462 \[hep-ex\]](#).
- [81] CMS Collaboration, A. M. Sirunyan *et al.*, “Search for heavy neutral leptons in events with

- three charged leptons in proton-proton collisions at $\sqrt{s} = 13$ TeV,” *Phys. Rev. Lett.* **120** no. 22, (2018) 221801, [arXiv:1802.02965 \[hep-ex\]](#).
- [82] **DELPHI** Collaboration, P. Abreu *et al.*, “Search for neutral heavy leptons produced in Z decays,” *Z. Phys.* **C74** (1997) 57–71. [Erratum: *Z. Phys.*C75,580(1997)].
- [83] G. Cottin, J. C. Helo, and M. Hirsch, “Displaced vertices as probes of sterile neutrino mixing at the LHC,” [arXiv:1806.05191 \[hep-ph\]](#).
- [84] S. Alekhin *et al.*, “A facility to Search for Hidden Particles at the CERN SPS: the SHiP physics case,” *Rept. Prog. Phys.* **79** no. 12, (2016) 124201, [arXiv:1504.04855 \[hep-ph\]](#).
- [85] **CMS** Collaboration, “First Level Track Jet Trigger for Displaced Jets at High Luminosity LHC,” Tech. Rep. CMS-PAS-FTR-18-018, CERN, Geneva, 2018.
<http://cds.cern.ch/record/2647987>.
- [86] J. Alimena *et al.*, “Searching for long-lived particles beyond the Standard Model at the Large Hadron Collider,” [arXiv:1903.04497 \[hep-ex\]](#).
- [87] J. Liu, Z. Liu, and L.-T. Wang, “Enhancing Long-Lived Particles Searches at the LHC with Precision Timing Information,” *Phys. Rev. Lett.* **122** no. 13, (2019) 131801, [arXiv:1805.05957 \[hep-ph\]](#).